DYNAMIC ANALYSIS OF TWO-LINK FLEXIBLE MANIPULATOR USING FEM UNDERGOING BENDING-TORSIONAL VIBRATIONS

Natraj MISHRA, S.P. SINGH

Abstract- *In this paper, a two-link flexible manipulator is analyzed using finite element approach whose links are undergoing combined bending and torsional vibrations. Mathematical model of the flexible manipulator is obtained using Lagrangian dynamics. The links are modelled as Euler-Bernoulli beams and discretized using 'space-frame' and 'plane-frame' elements. The present work deals with various non-linear effects like, coupling between rigid and flexible degrees of freedom, centrifugal and Coriolis effects and presence of gravity. The mathematical model is validated using results available in the literature. The novelty of the present work lies in inclusion of torsional effects and thus highlighting their effects on positional accuracy of the flexible manipulator.*

Keywords- *Lagrangian-FEM, coupled bending-torsion vibrations, coupled rigid and flexible motions, Flexible manipulator, frequency analysis*

1. INTRODUCTION

Accurate modelling and control of flexibility in robots is a challenging task. Many researchers are working towards achieving the positional accuracy of such robots. If these unwanted vibrations are reduced then definitely, less inertia torque will be required to drive them. This will ultimately lead to the reduction of power consumption by the motors used to drive them. A comprehensive literature review has been done by Benosman and Vey [1]

and Dwivedy and Eberhard [2] in the area of *flexible* robotics. They have compiled various research papers dealing with the modelling and control of *flexible* robots. Many researchers have contributed towards area of *flexible* robotics. Most of them have used Lagrangian dynamics for modelling the *flexible* manipulators. They have treated the *links* of the manipulator as Euler-Bernoulli beams. Table 1 highlights the contribution of these researchers in chronological order.

**Table 1: Significant work done by few authors in the area of Flexible Robotics using the approach of FEM**

S.No.	Researchers	Work Done	Year
1	Sunada and Dubowsky [3]	They used component mode synthesis to reduce the number of differential equations resulting from FEM.	1981
2.	Dado and Soni [4]	They carried both the forward and inverse dynamic analyses of elastic manipulators.	1986
3.	Nagnathan and Soni [5]	Only these researchers have used Newton-Euler approach; the *links* are also modelled as Timoshenko beams.	1986
4.	Usoro et al. [6]	They have considered the effect of gravity for the first time.	1986
5.	Bayo [7]	He found the *joint* torque for producing a desired tip motion of the *flexible link*. He also analysed the *flexible* manipulator in 'frequency domain'.	1987
6.	Simo and Vu-Quoc [8]	They used non-linear beam theory for modelling the *flexible* structures and highlighted its significance in transient analysis.	1987
7.	Tzou and Wan [9]	They introduced Rayleigh's and viscoelastic dampings during the mathematical modelling of *flexible* manipulators.	1990
8.	Chedmail et al. [10]	They introduced active damping for controlling the vibrations of *flexible links*. They made use of Linear Quadratic Regulator for controlling	1991

		vibrations. Two-Link Flexible manipulator is considered for the first time.	
9.	Alberts et al. [11]	They have considered the effectiveness of viscoelastic damping in curbing the vibrations of *flexible links*.	1992
10.	Gaultier and Cleghorn [12]	They applied FEM on *links* which have both rotating and translating motions. Thus, they extended the work of previous authors by including prismatic motion.	1992
11.	Hu and Ulsoy [13]	They have provided a model for the design of a controller for a Rigid-flexible spherical-coordinate robot.	1994
12.	Stylianou and Tabarrok	They modelled an axially moving beam using 'variable-domain finite beam elements' [14] and also investigated its dynamic stability [15].	1994
13.	Theodore and Ghosal [16]	They discussed the robustness and stability issues of the *flexible links*.	2003
14.	Fotouhi [17]	They analysed the *flexible* robots undergoing large deformations.	2007

A comparison between the 'assumed modes method' (AMM) and the 'finite elements method' (FEM) for modelling *flexible multi-link* manipulators was done by Meghdari and Ghassempouri [18] and Theodore and Ghosal [19]. They concluded that the use of FEM is recommended for manipulator *links* with complex geometries and having flexibilities and the use of AMM for manipulator *links* with uniform geometries.

2. MATHEMATICAL MODELLING

An accurate dynamic model of a Two-link Flexible manipulator having two revolute *joints* undergoing both small bending and small torsional deformations is prepared. Fig. 1 shows a Two-Link Flexible manipulator undergoing both bending and torsional deformations along with *rigid* revolutions at their *joints*. Plane X-Y is the plane of bending while plane Y-Z is the plane of torsion.
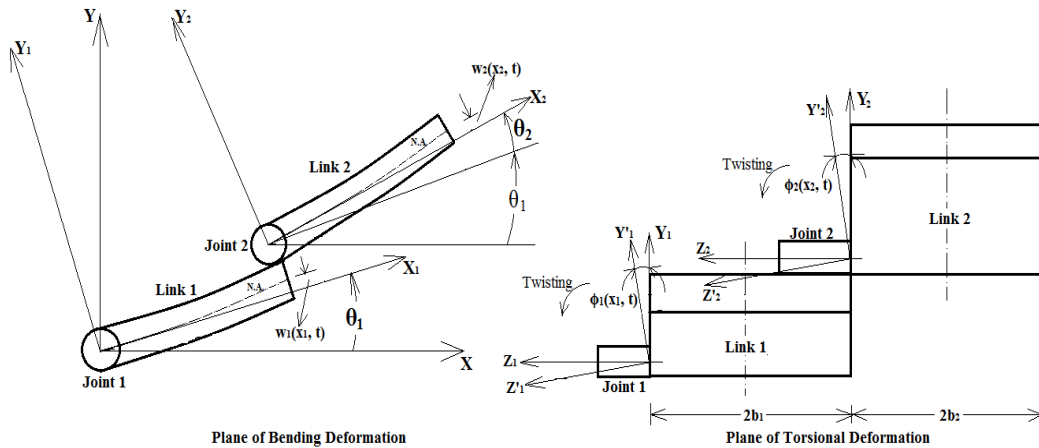
Fig. 1: Dynamic analysis of Two-Link Flexible manipulator undergoing both bending and torsional deformations.

In figure 1, X-Y-Z is the reference/ ground frame while X_1-Y_1-Z_1 and X_2-Y_2-Z_2 are the local frames attached to Link-1 and Link-2 respectively. Axis X_1 is aligned along the un-deformed neutral axis (N.A.) of Link-1 while axis X_2 is aligned along the un-deformed neutral axis of Link-2. The origins of these local frames are located at Joint-1 and Joint-2 respectively. Joint-1 is given a *rigid* rotation of θ_1 and Joint-2 is given a *rigid* rotation of θ_2. The position of any point on Link-1 with respect to ground is given by:

$$\{p_1\} = [T_1][T_{1T}]\{r_{1T}\} + [T_1]\{r_1\} \quad (1)$$

Similarly, the position of any point on Link-2 with respect to ground is given by:

$$\{p_2\} = [T_1]\{r_1^*\} + [T_1][T_{1T}^*]\{r_{1T}^*\} + [T_A^*][T_1][T_2]\{r_2\} + [T_1][T_2][T_{2T}]\{r_{2T}\}$$
(2)

In above expressions,

$$T_1 = \begin{bmatrix} \cos\theta_1 & -\sin\theta_1 & 0 \\ \sin\theta_1 & \cos\theta_1 & 0 \\ 0 & 0 & 1 \end{bmatrix};$$

$$T_2 = \begin{bmatrix} \cos\theta_2 & -\sin\theta_2 & 0 \\ \sin\theta_2 & \cos\theta_2 & 0 \\ 0 & 0 & 1 \end{bmatrix};$$

$$\{r_1\} = \begin{Bmatrix} x_1 \\ w_1(x_1, t) \\ 0 \end{Bmatrix};$$

$$\{r_1^*\} = \begin{Bmatrix} L_1 \\ w_1(L_1, t) \\ 0 \end{Bmatrix}; \{r_2\} = \begin{Bmatrix} x_2 \\ w_2(x_2, t) \\ 0 \end{Bmatrix};$$

$$T_A^* = \begin{bmatrix} \cos(w_1^{*\prime}) & -\sin(w_1^{*\prime}) & 0 \\ \sin(w_1^{*\prime}) & \cos(w_1^{*\prime}) & 0 \\ 0 & 0 & 1 \end{bmatrix};$$

$$\{r_{iT}\} = \{0 \quad b_i\phi_i \quad b_i\}' \; ;$$

$$\{r_{iT}^*\} = \{0 \quad b_i\phi_i^* \quad b_i\}' \; ;$$

$$\{g\}' = \{0 \quad g \quad 0\} \; ;$$

$$[T_{iT}] = \begin{bmatrix} 1 & 0 & 0 \\ 0 & \cos\phi_i & -\sin\phi_i \\ 0 & \sin\phi_i & \cos\phi_i \end{bmatrix};$$

$$[T_{iT}^*] = \begin{bmatrix} 1 & 0 & 0 \\ 0 & \cos\phi_i^* & -\sin\phi_i^* \\ 0 & \sin\phi_i^* & \cos\phi_i^* \end{bmatrix} \; ; \quad (3)$$

L_1 and L_2 = lengths of Link-1 and Link-2 respectively,

θ_1 and θ_2 = *joint* rotations (rigid) of Joint-1and Joint-2 respectively,

x_1 and x_2 = distances measured along un-deformed Link-1 and Link-2 axes, i.e. X_1 and X_2 respectively,

$w_1(x_1, t)$ and $w_2(x_2, t)$ = elastic displacements of Link-1 and Link-2 respectively undergoing bending vibrations

$w_1^{*\prime}$ = bending angle at end point of Link-1 = $\frac{dw_1^*}{dx_1}$

$\{r_1\}$ = position coordinates of any point on Link-1 w.r.t to un-deformed Link-1 axis i.e., X_1 in plane X_1-Y_1

$\{r_2\}$ = position coordinates of any point on Link-2 w.r.t to un-deformed Link-2 axis i.e., X_2 in plane X_2-Y_2

$\{r_1^*\}$ = position coordinates of end point of Link-1 w.r.t. un-deformed beam-1 axis X_1 in plane X_1-Y_1

$\{r_{iT}\}$ = position coordinates of any point on Link-i in plane Y_i-Z_i

$\phi_i = \phi_i(x_i, t)$ = torsional deformation of any point on Link-i

$\phi_i^* = \phi_i(L_i, t)$ = torsional displacement of end point of Link-i; *i* represents the *link* number (*i* = 1 and 2)

The total kinetic energy of the manipulator system is given by:

$$K.E.= \frac{1}{2}\rho_1 A_1 \int_0^{L_1}\{\dot{p}_1\}'\{\dot{p}_1\}dx_1 + \frac{1}{2}\rho_2 A_2 \int_0^{L_2}\{\dot{p}_2\}'\{\dot{p}_2\}dx_2 \qquad (4)$$

Total potential energy of the manipulator system is given by:

$$P.E.= \frac{E_1 I_1}{2}\int_0^{L_1}\left(\frac{\partial^2 w_1^2}{\partial x_1^2}\right)^2 dx_1 + \frac{G_1 J_1}{2}\int_0^{L_1}\left(\frac{\partial \phi_1}{\partial x_1}\right)^2 dx_1 +$$
$$\rho_1 A_1 \int_0^{L_1}\{g\}'\{p_1\}dx_1 +$$
$$\frac{E_2 I_2}{2}\int_0^{L_2}\left(\frac{\partial^2 w_2^2}{\partial x_2^2}\right)^2 dx_2 + \frac{G_2 J_2}{2}\int_0^{L_2}\left(\frac{\partial \phi_2}{\partial x_2}\right)^2 dx_2 +$$
$$\rho_2 A_2 \int_0^{L_2}\{g\}'\{p_2\}dx_2 \qquad (5)$$

In equations- 4 and 5, J_1 and J_2 are the polar moment of inertias of Link-1 and Link-2 respectively. The *joint* torques can be obtained using Lagrangian dynamics as follows:

$$\frac{d}{dt}\left(\frac{\partial \mathcal{L}}{\partial \dot{q}}\right) - \frac{\partial \mathcal{L}}{\partial q} = F \qquad (6)$$

In above expression, $\mathcal{L}$ represents Lagrangian of the system and is obtained by taking the difference of total kinetic energy and total potential energy of the system; *q* represents generalized coordinates and *F* represents generalized torque/force.

$$q = \{\theta_1 \quad \theta_2 \quad w_1 \quad w_1^* \quad w_2 \quad w_2^* \quad \phi_1 \quad \phi_1^* \quad \phi_2 \quad \phi_2^*\}' \qquad (6a)$$
$$F = \{\tau_1 \quad \tau_2 \quad 0 \quad 0 \quad 0 \quad 0 \quad 0 \quad 0 \quad 0 \quad 0\}' \qquad (6b)$$

3. DISCRETIZATION USING FINITE ELEMENTS METHOD

In this paper, FEM is used to model the vibratory motions of the *flexible links*. This involves division of *flexible links* into some finite number of elements and finding the inertia and stiffness matrices that govern the dynamics of the system under consideration. Figure 2 (provided at the end) shows the discretization of *flexible links* using two Space-Frame Elements [20]. A 'space-frame element' has two nodes with each node having six degrees of freedom: three translational (Q_{6i-5},

Q_{6i-4} and Q_{6i-3}) and three rotational (Q_{6i-2}, Q_{6i-1} and Q_{6i}). The complete equation of motion of the *flexible* manipulator is given by equation (7a).

$$\begin{bmatrix} M_{rr} & M_{rf} \\ M_{fr} & M_{ff} \end{bmatrix}_{(n+N) \, X \, (n+N)} \begin{Bmatrix} \ddot{q}_r \\ \ddot{q}_f \end{Bmatrix}_{(n+N) \, X \, 1} +$$

$$\begin{bmatrix} 0 & 0 \\ 0 & K_{ff} \end{bmatrix}_{(n+N) \, X \, (n+N)} \begin{Bmatrix} q_r \\ q_f \end{Bmatrix}_{(n+N) \, X \, (n+N)} +$$

$$\begin{bmatrix} H \\ 0 \end{bmatrix}_{(n+N) \, X \, 1} + \begin{bmatrix} G \\ 0 \end{bmatrix}_{(n+N) \, X \, 1} = \begin{Bmatrix} F_r \\ F_f \end{Bmatrix}_{(n+N) \, X \, 1}$$

(7a)

In equation (7a), subscripts- *r* and *f* stand for *rigid* and *flexible* respectively. *N* represents the *rigid* degrees of freedom present in the system and *n* represents the *flexible* degrees of freedom obtained from finite element formulation. For the present case, since there are two *flexible links*, we have *N* = 2. Hence, M_{rr} consists of two diagonal elements- M_{11} and M_{22}. M_{rf} and M_{fr} represent the coupling between *rigid* and *flexible* motions.

$$M_{fr} = M'_{rf} \tag{7b}$$

One finite element per *link* is considered for the present analysis. Thus, there are three nodes and eighteen degrees of freedom (i.e., n = 18). The first six degrees of freedom are considered to be fixed. Hence, there remain only twelve degrees of freedom. Thus, we get

$$M_{ff} = [m^e]_{12X12} \tag{7c}$$

If there are two finite elements per *link* then there will be four elements in total having five nodes. The total degrees of freedom will be thirty then (i.e., n = 30). In the similar fashion, we can obtain the elements of stiffness matrix also. For the present case,

$$K_{ff} = [k^e]_{12X12} \tag{7d}$$

$$F_r = \begin{Bmatrix} \tau_1 \\ \tau_2 \end{Bmatrix} \tag{7e}$$

τ_1 and τ_2 represent *joint* torques.

For vibration analysis of the *flexible links*, it is necessary to find out the Global stiffness matrix and Global mass matrix. The equation of motion for undamped vibrations for 'n' degrees of freedom is as follows:

$$[M_{ff}]_{n\times n}\{\ddot{q}_f\}_{n\times 1} + [K_{ff}]_{n\times n}\{q_f\}_{n\times 1} = \{F_f\}_{n\times 1} \tag{8a}$$

where, M_{ff} = global mass matrix,
K_{ff} = global stiffness matrix,

F_f = global force vector, and
q_f = vector of global degrees of freedom.
If damping is present within the system, then the equation of motion for vibratory motion will be written as follows:

$$[M_{ff}]_{n\times n}\{\ddot{q}_f\}_{n\times 1} + [C_{ff}]_{n\times n}\{\dot{q}_f\}_{n\times 1} + [K_{ff}]_{n\times n}\{q_f\}_{n\times 1} = \{F_f\}_{n\times 1} \tag{8b}$$

where, C_{ff} = global damping matrix.
In local frame, the stiffness matrix of a Space-frame element is given by:

$$k'_e = \begin{bmatrix} k'_{11e} & k'_{12e} \\ k'_{21e} & k'_{22e} \end{bmatrix} \tag{8c}$$

$$k'_{11e} = \begin{bmatrix} AS & 0 & 0 & 0 & 0 & 0 \\ 0 & a_z & 0 & 0 & 0 & b_z \\ 0 & 0 & a_y & 0 & -b_y & 0 \\ 0 & 0 & 0 & TS & 0 & 0 \\ 0 & 0 & -b_y & 0 & c_y & 0 \\ 0 & b_z & 0 & 0 & 0 & c_z \end{bmatrix};$$

$$k'_{12e} = \begin{bmatrix} -AS & 0 & 0 & 0 & 0 & 0 \\ 0 & -a_z & 0 & 0 & 0 & b_z \\ 0 & 0 & -a_y & 0 & -b_y & 0 \\ 0 & 0 & 0 & -TS & 0 & 0 \\ 0 & 0 & b_y & 0 & d_y & 0 \\ 0 & -b_z & 0 & 0 & 0 & d_z \end{bmatrix};$$

$$k'_{21e} = \begin{bmatrix} -AS & 0 & 0 & 0 & 0 & 0 \\ 0 & -a_z & 0 & 0 & 0 & -b_z \\ 0 & 0 & -a_y & 0 & b_y & 0 \\ 0 & 0 & 0 & -TS & 0 & 0 \\ 0 & 0 & -b_y & 0 & d_y & 0 \\ 0 & b_z & 0 & 0 & 0 & d_z \end{bmatrix};$$

$$k'_{22e} = \begin{bmatrix} AS & 0 & 0 & 0 & 0 & 0 \\ 0 & a_z & 0 & 0 & 0 & -b_z \\ 0 & 0 & a_y & 0 & b_y & 0 \\ 0 & 0 & 0 & TS & 0 & 0 \\ 0 & 0 & b_y & 0 & c_y & 0 \\ 0 & -b_z & 0 & 0 & 0 & c_z \end{bmatrix}$$

In above matrices, $AS = \frac{EA_e}{l_e}$; $a_z = \frac{12EI_z}{l_e^3}$; $a_y = \frac{12EI_y}{l_e^3}$; $b_z = \frac{6EI_z}{l_e^2}$; $b_y = \frac{6EI_y}{l_e^2}$; $c_z = \frac{4EI_z}{l_e}$; $c_y = \frac{4EI_y}{l_e}$; $d_z = \frac{2EI_z}{l_e}$; $d_y = \frac{2EI_y}{l_e}$; $TS = \frac{GJ_e}{l_e}$ (8d)

where, E = Young's modulus of the element; G = modulus of rigidity of the element; A_e = area of cross-section of the element; l_e = length of the element; I_y and I_z are area moment of inertias of the element about *y*- and *z*-axes respectively, J_e = polar area moment of inertia of the element. The mass matrix of Space-frame element in local frame is given by

equations- (8e) and (8f) given at the end of the paper. The local force vector is represented by equation (8g) provided at the end. In global frame, we have

$$Global\ stiffness\ matrix, k^e = L^T k_e' L$$
(8h)

$$Global\ force\ vector, F_f = L^T f' \quad (8i)$$

$$Global\ mass\ matrix, m^e = L^T m_e' L$$
(8j)

where, L is the transformation matrix and is given by:

$$L = \begin{bmatrix} \lambda & 0 & 0 & 0 \\ 0 & \lambda & 0 & 0 \\ 0 & 0 & \lambda & 0 \\ 0 & 0 & 0 & \lambda \end{bmatrix}$$
(8k)

λ is the matrix of direction cosines and is given as follows:

$$\lambda = \begin{bmatrix} l_1 & m_1 & n_1 \\ l_2 & m_2 & n_2 \\ l_3 & m_3 & n_3 \end{bmatrix}$$
(8l)

In above matrix, l_1, m_1 and n_1 represent the direction cosines of local-X axis of the Space-frame element w.r.t. global frame. Similarly, l_2, m_2 and n_2 represent the direction cosines of local-Y axis and l_3, m_3 and n_3 represent the direction cosines of local-Z axis. The conversion between local degrees of freedom (Q_l) of the element and the global degrees of freedom (Q) can be done using the relation:

$$\{Q_l\}_{12\times1} = [L]_{12\times12}\{Q\}_{12\times1} \quad (8m)$$

4. RESULTS

The results are obtained in two ways. In the first case, the coupling between *rigid* and *flexible* motions is considered. In the second case, results are obtained by neglecting this coupling. Firstly, results are obtained for bending vibrations only. After that torsional effects are also considered.

4.1 Results using bending vibrations only
4.1.1: Effect of coupling between Rigid and Flexible motions

In this case, Plane-frame element is used. The generalized coordinates and generalized forces will be represented as follows:

$$q = \{\theta_1 \quad \theta_2 \quad w_1 \quad w_2 \quad w_1^*\}' \quad (9a)$$
$$F = \{\tau_1 \quad \tau_2 \quad 0 \quad 0 \quad 0\}' \quad (9b)$$

The mass matrix M(q) will be of order 5x5. The coefficients representing the elements in the first two rows of the inertia matrix

$[M_j(t)]_{5\times5}$ (j = *joint* number = 1 and 2) are evaluated using the following expressions.

$$M_{11} = \frac{1}{2}\rho_1 A_1 \left[\frac{2}{3}L_1^3 + \int_0^{L_1} w_1^2 dx_1\right] +$$
$$\frac{1}{2}\rho_2 A_2 \left[2L_2(L_1^2 + w_1^{*2}) + \frac{2}{3}L_2^3 +\right.$$
$$2\int_0^{L_2} w_2^2 dx_2 + 2L_2^2(L_1\cos\theta_2 + w_1^*\sin\theta_2) +$$
$$\left. 4(w_1^*\cos\theta_2 - L_1\sin\theta_2)\int_0^{L_2} w_2 dx_2\right];$$
(10a)

$$M_{12} = \frac{1}{2}\rho_2 A_2 \left[L_2^2(L_1\cos\theta_2 + w_1^*\sin\theta_2) +\right.$$
$$\frac{2}{3}L_2^3 + 2\int_0^{L_2} w_2^2 dx_2 + 2(w_1^*\cos\theta_2 -$$
$$\left. L_1\sin\theta_2)\int_0^{L_2} w_2 dx_2\right];$$
(10b)

$$M_{13} = \frac{1}{2}\rho_1 A_1 L_1^2;$$
(10c)

$$M_{14} = \frac{1}{2}\rho_1 A_1 L_2^2;$$
(10d)

$$M_{15} = \frac{1}{2}\rho_2 A_2 \left[2L_1 L_2 + L_2^2\cos\theta_2 -\right.$$
$$\left. 2\sin\theta_2 \int_0^{L_2} w_2 dx_2\right];$$
(10e)

$$M_{21} = M_{12};$$
(10f)

$$M_{22} = \frac{1}{2}\rho_2 A_2 \left(\frac{2}{3}L_2^3 + 2\int_0^{L_2} w_2^2 dx_2\right);$$
(10g)

$$M_{23} = 0;$$
(10h)

$$M_{24} = \left(\frac{-1}{2}\right)\rho_2 A_2 L_2^2;$$
(10i)

$$M_{25} = \frac{1}{2}\rho_2 A_2 \left[-L_2^2\cos\theta_2 +\right.$$
$$\left. 2\sin\theta_2 \int_0^{L_2} w_2 dx_2\right];$$
(10j)

The above expressions were derived using Lagrangian dynamics [21]. The same equations are used while obtaining the response of the *flexible* manipulator using FEM. The only difference is that while using FEM, the integration sign is replaced by the summation sign. This is because; in FEM the system is divided into finite elements having nodes. Complete focus is now upon the nodes. By increasing the number of finite elements, number of nodes increase, size of the elements decrease and hence the accuracy of the solution increases. Equation (7a) is used to obtain the results. One finite element per *link* is considered for the present analysis. Thus, there are three nodes and nine degrees of freedom (n = 9).

$$M_{ff} = [m^e]_{9\times9} \quad (11a)$$

$$M_{rf} = \begin{bmatrix} 0 & M_{13} & 0 & 0 & M_{15} & 0 & 0 & M_{14} & 0 \\ 0 & M_{23} & 0 & 0 & M_{25} & 0 & 0 & M_{24} & 0 \end{bmatrix}$$

(11b)

The first three degrees of freedom are considered to be fixed. Hence, there remain only six degrees of freedom. Thus, we get

$$M_{ff} = [m^e]_{6\times6} \tag{11c}$$

$$M_{rf} = \begin{bmatrix} 0 & M_{13} & 0 & 0 & M_{13} & 0 & 0 \\ 0 & M_{23} & 0 & 0 & M_{23} & 0 & 0 \end{bmatrix}$$

The first three degrees of freedom are fixed. Hence, first three columns from both the rows are eliminated. Similarly for the present case we obtain,

$$K_{ff} = [k^e]_{6\times6} \tag{11g}$$

$$F_r = \begin{Bmatrix} \tau_1 \\ \tau_2 \end{Bmatrix} \tag{11h}$$

$$F_f = \boldsymbol{L}_{pf}^T\begin{bmatrix} 0 & \frac{pl_e}{2} & \frac{pl_e^2}{12} & 0 & \frac{pl_e}{2} & \frac{-pl_e^2}{12} \end{bmatrix}^T$$

(11i)

p = distributed load on *links* and is due to presence of gravity only.

$$\boldsymbol{L}_{pf} = \begin{bmatrix} \boldsymbol{\lambda}_{pf} & 0 \\ 0 & \boldsymbol{\lambda}_{pf} \end{bmatrix}; \tag{11j}$$

$$\boldsymbol{\lambda}_{pf} = \begin{bmatrix} \cos\theta_1 & \sin\theta_1 & 0 \\ -\sin\theta_1 & \cos\theta_1 & 0 \\ 0 & 0 & 1 \end{bmatrix} \text{ for Link-1,}$$

and (11j)

$$\boldsymbol{\lambda}_{pf} = \begin{bmatrix} \cos(\theta_1+\theta_2) & \sin(\theta_1+\theta_2) & 0 \\ -\sin(\theta_1+\theta_2) & \cos(\theta_1+\theta_2) & 0 \\ 0 & 0 & 1 \end{bmatrix}$$

for Link-2. (11k)

The physical parameters of the manipulator are tabulated in Table 2. These parameters are used to obtain the simulation results.

$$M_{rf} = \begin{bmatrix} 0 & M_{15} & 0 & 0 & M_{14} & 0 \\ 0 & M_{25} & 0 & 0 & M_{24} & 0 \end{bmatrix}$$

(11d)

If there are two finite elements per *link* then there will be four elements in total having five nodes. The total degrees of freedom will be fifteen then. The matrix M_{rf} will then be written as given in equation (11f).

$$M_{rf} = \begin{bmatrix} M_{15} & 0 & 0 & M_{14} & 0 & 0 & M_{14} & 0 \\ M_{25} & 0 & 0 & M_{24} & 0 & 0 & M_{24} & 0 \end{bmatrix}$$ (11f)

Viscoelastic damping [22] is incorporated within the model of *flexible* manipulator. For this, Kelvin-Voigt elements are considered.

Table 2: Physical parameters for Two-Link Flexible manipulator undergoing bending vibrations

| Physical parameter	Value
Length of both the *links*, L_1 and L_2	1 m
Flexural rigidity of both the *links*	5.68 X 10^6 Nm^2
Area of cross-section of both the *links*	0.0419 m^2
Density of both the *links*	7850 kg/m^3
Joint-1 torque	0.1 Nm (step)
Joint-2 torque	0.01 Nm (step)
Type of element	Plane-frame element
Mode of damping	Viscoelastic damping using Kelvin-Voigt elements
Solver	*Ode45*

The simulation results are shown below (Fig. 3 to Fig. 5) in the form of graphs. These graphs represent the tip velocities of second *link* of the *flexible* manipulator.
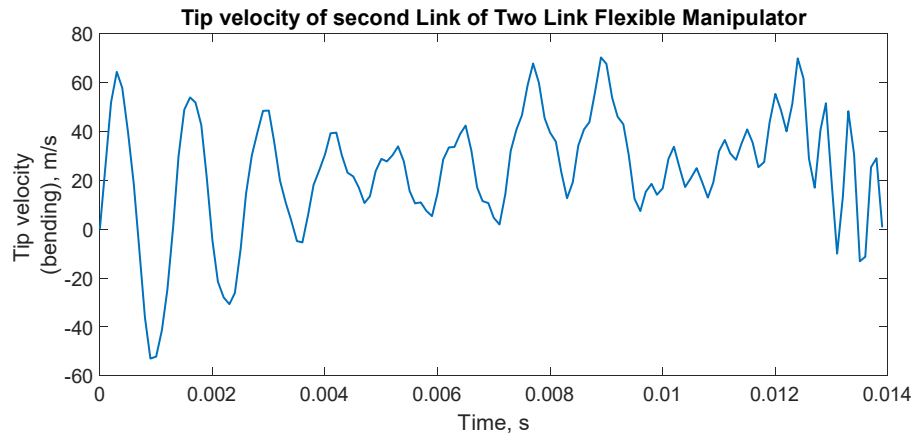
Fig. 3: Tip velocity of the second *link* of Two-Link Flexible manipulator undergoing bending vibrations (Coupling between *rigid* and *flexible* motions is considered.)

Fig. 3 is obtained after solving equation (7a). The simulation stops after 0.018 second. This is because of the presence of coupling between *rigid* and *flexible* motions in equation (7a). If centrifugal and Coriolis terms are present then the simulation does not run. Step size of '0.1 ms' was used to obtain the above graph. When the coupling terms are reduced (say by a factor of 10000) the simulation runs for a longer duration. This can be observed from the following graphs.
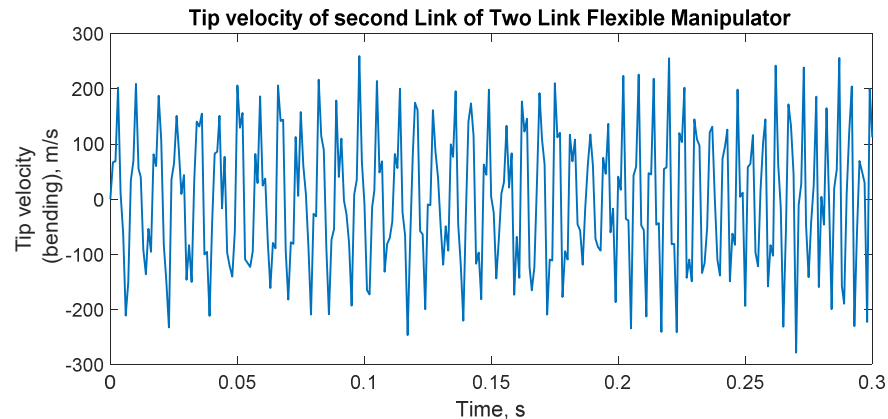
Fig. 4: Tip velocity of the second *link* of Two-Link Flexible manipulator undergoing bending vibrations (Coupling between *rigid* and *flexible* motions is reduced by 10000.)

In Figure 4, it can be seen that tip velocity is high. The effect of centrifugal and Coriolis torques are considered while obtaining the above results. The simulation stopped after 0.336 second. Step size of '1 ms' was used to obtain the above graph.
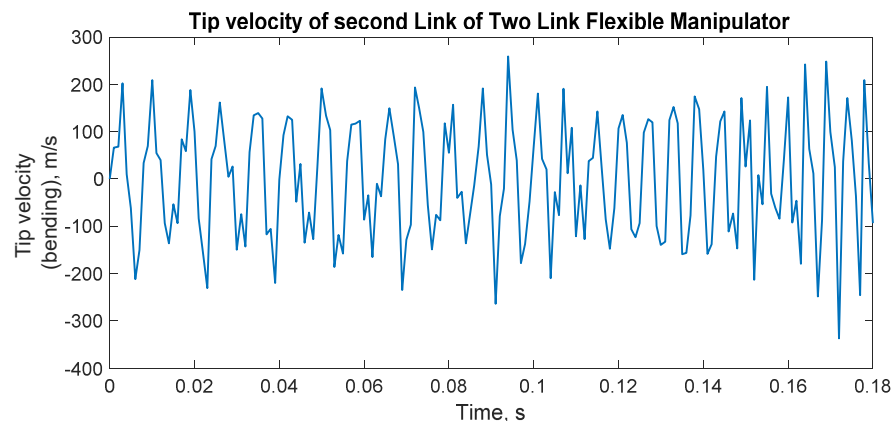
Fig. 5: Tip velocity of the second *link* of Two-Link Flexible manipulator undergoing bending vibrations (Coupling between *rigid* and *flexible* motions is reduced by 10000; effect of gravity is considered.)

Figure 5 shows the tip velocity of second *link* of the *flexible* manipulator when the effect of gravity is considered along with the centrifugal and Coriolis torques. Step size of '1 ms' was used. It is found that due to presence of gravity, the simulation stopped after 0.207 second: earlier than the previous case. From the simulation results, it can be inferred that equation (7a) for the Two-link Flexible manipulator is highly non-linear.

4.1.2: Neglecting the effect of coupling between Rigid and Flexible motions

The presence of coupling between the *rigid* and *flexible* motions makes it difficult to solve equation (7a). Hence, in this case coupling is removed and then the effect on simulation is observed. Before that, few changes are done in the dynamics

of the system. Analytically, the vibrating motion of an Euler-Bernoulli beam is given by following equation.

$$\frac{\partial^2 w}{\partial t^2} + \left(\frac{EI}{\rho A}\right)\frac{\partial^4 w}{\partial x^4} = f(x,t) \quad (12)$$

In above equation, w = deflection of beam, E = Young's modulus of beam, I = area moment of inertia of beam, ρ = mass density of beam, A = area of cross-section of beam and f(x,t) = external force acting on the beam. The analytical solution of equation (12) can be obtained using the approach of AMM [23]. Since approach of FEM is followed in this paper, equation (12) can be discretized to yield equation (8a). The load vector F_f is now reformulated to contain two types of loads. First one is due to the distributed load described by equation (11i) and the second type of load is due to the excitation provided by the actuators placed at *joints*.

4.2 Calculation of excitation forces acting at the tips of the *links*

Fig. 6 (provided at the end) helps to understand the excitation forces acting at the tips of the *links*. These forces are calculated as follows.

$$f_{11} = \frac{\tau_1}{OA} = \frac{\tau_1}{L_1} \text{ (perpendicular to OA)}$$
$$(13a)$$

$$f_{22} = \frac{\tau_2}{AB} = \frac{\tau_2}{L_2} \text{ (perpendicular to AB)}$$
$$(13b)$$

$$f_{21} = \frac{\tau_1}{OB} \text{ (perpendicular to OB)} \quad (13c)$$

Net force acting at B (perpendicular to AB),
$$f_{bB} = f_{22} + f_{21}\cos(\theta_2\text{-}\phi) \quad (13d)$$
Net force acting at B (along AB), $f_{aB} = f_{21}\sin(\theta_2\text{-}\phi)$ (13e)

Hence, load vector for the element containing the tip of the given *link* as one of its nodes can be described as follows:

$$F_f = \boldsymbol{L}_{pf}^T\left[0 \quad \frac{ple}{2} \quad \frac{pl_e^2}{12} \quad 0 \quad \frac{ple}{2}+f_{11} \quad \frac{-pl_e^2}{12}\right]^T \text{ for Link-1, and} \quad (13f)$$

$$F_f = \boldsymbol{L}_{pf}^T\left[0 \quad \frac{ple}{2} \quad \frac{pl_e^2}{12} \quad 0+f_{aB} \quad \frac{ple}{2}+f_B \quad \frac{-pl_e^2}{12}\right]^T \text{ for Link-2.} \quad (13g)$$

The load vectors for remaining elements remain same as provided by equation (11i). Since, torsional vibrations are not considered here, hence the axes Z-Z_1 and Z-Z_2 (Fig. 1) will always be parallel to each other. The load vector can be described in another way as follows:

$$F_f = \boldsymbol{L}_{pf}^T\left[0 \quad \frac{p_y le}{2} \quad \frac{p_y l_e^2}{12} \quad 0 \quad \frac{p_y le}{2} \quad \frac{-p_y l_e^2}{12}-\tau_1\right]^T$$
for Link-1, and $\quad (13h)$

$$F_f = \boldsymbol{L}_{pf}^T\left[0 \quad \frac{p_y le}{2} \quad \frac{p_y l_e^2}{12} \quad 0 \quad \frac{p_y le}{2} \quad \frac{-p_y l_e^2}{12}-\tau_1-\tau_2\right]^T$$
for Link-2. $\quad (13i)$

It is to be noted that the load vectors described in equation (13f) to equation (13i) are only for the last elements of Link-1 and Link-2 respectively. Figure 7 shows the tip velocity of second *link* of the *flexible* manipulator when coupling between *rigid* and *flexible* motions are not considered.
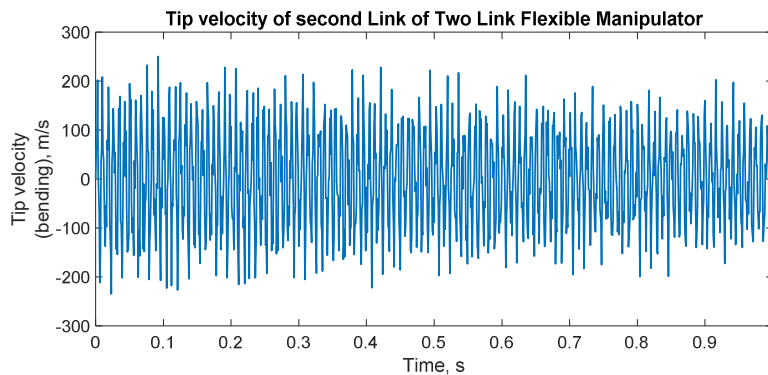
Fig. 7: Tip velocity of the second *link* of Two-Link Flexible manipulator undergoing bending vibrations (Coupling between *rigid* and *flexible* motions is not considered; effect of gravity is not considered.).

In Figure 7, effect of gravity is not considered while the effect of centrifugal and Coriolis torques are taken into account. It can be observed that the simulation runs for a longer duration of time. After observing the simulation results from Fig. 3 to Fig. 7, it can be concluded that the Two-Link Flexible manipulator is a highly non-linear system due to the presence of coupling between *rigid* and *flexible* motions, presence of gravity and presence of centrifugal and Coriolis terms in the equation of motion (equation 7a).

4.3 Results using combined bending-torsion vibrations

After obtaining results for bending vibrations, torsional effects are also included. Thus, the following results are for combined bending-torsional vibrations. For this, Space-frame elements are used. Damping is not considered while obtaining these results.

Equations- 13a to 13i describe the tip forces and tip load vectors. In case of coupled bending-torsion vibrations some additional forces will also act at the tips. Following equation describes the force acting at the tip of first *flexible link*, responsible for torsional vibrations.

$Twisting\ torque\ at\ tip\ of\ Link - 1,\ T_{w1} = f_{11}X\frac{1}{2}(2b_1 + 2b_2)$ (14)

Table 3: Physical parameters for Two-Link Flexible manipulator undergoing combined bending-torsional vibrations

| Physical parameter	Value
Length of both the *links*, L_1 and L_2	0.5 m
Flexural rigidity of Link-1 (E_1I_{1y} and E_1I_{1z})	14.93 Nm^2
Flexural rigidity of Link-2 (E_2I_{2y} and E_2I_{2z})	1.017 Nm^2
Area of cross-section of Link-1	4 cm x 4 mm
Area of cross-section of Link-2	5.17 cm x 1.5 mm
Density of both the *links*	7850 kg/m^3
Modulus of rigidity of both the *links*	8.08 x 10^{11} N/m^2
Joint-1 torque	Square wave of amplitude 0.05 Nm and time period 0.1s
Joint-2 torque	Square wave of amplitude 0.01 Nm and time period 0.1s
Type of finite element used	Space-frame element
Solver	*Ode45*

This twisting torque acts perpendicular to plane: Y_1-Z_1, i.e. along X_1 axis (refer to Fig. 6 and Fig. 1). This torque vector when seen from global frame (axes: X-Y-Z in Fig. 1) will have two rectangular components along X-axis and Y-axis. Besides that, gyroscopic couples will also act on the tips. The expressions for gyroscopic couple are given as follows.

$Gyroscopic\ couple\ at\ tip\ of\ Link - 1,\ GC_1 = J_{m1}\dot{\phi}_1(\dot{\theta}_1 + \dot{\gamma}_1)$ (15a)

The couple GC$_1$ will act along Y_1-axis; $\dot{\phi}_1$ represents the rate of twist of Link-1 about local X_1-axis, $\dot{\gamma}_1$ represents the rate of change of slope of tip of Link-1 due to bending about Z_1-axis and J_{m1} is the mass moment of inertia of Link-1.

$Gyroscopic\ couple\ at\ tip\ of\ Link - 2,\ GC_2 = J_{m2}(\dot{\phi}_2 - \dot{\phi}_1\cos\theta_2)(\dot{\theta}_1 + \dot{\gamma}_1 + \dot{\theta}_2 + \dot{\gamma}_2)$ (15b)

The couple GC$_2$ will act along Y_2-axis; $\dot{\phi}_2$ represents the rate of twist of Link-2 about local X_2-axis, $\dot{\gamma}_2$ represents the rate of change of slope of tip of Link-2 due to bending about Z_2-axis and J_{m2} is the mass moment of inertia of Link-2. The local force vectors for the elements containing tips of the *links* as one of their nodes are given by equations- 15c and 15d provided at the end.
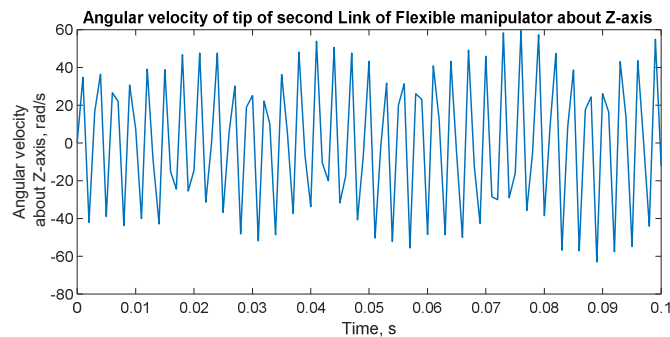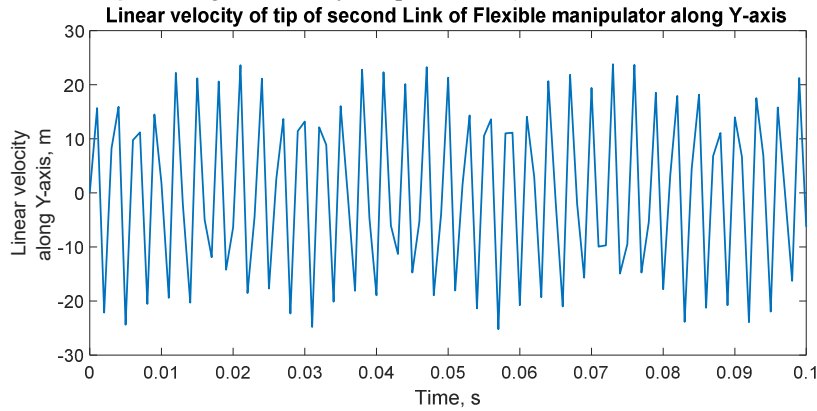

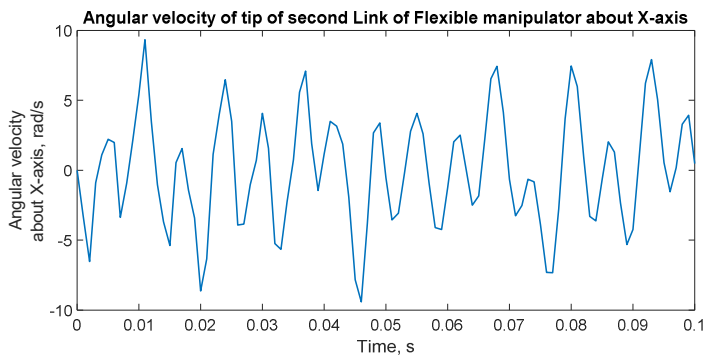**Fig. 8:** Angular velocity of tip of second *flexible link* about Z-axis

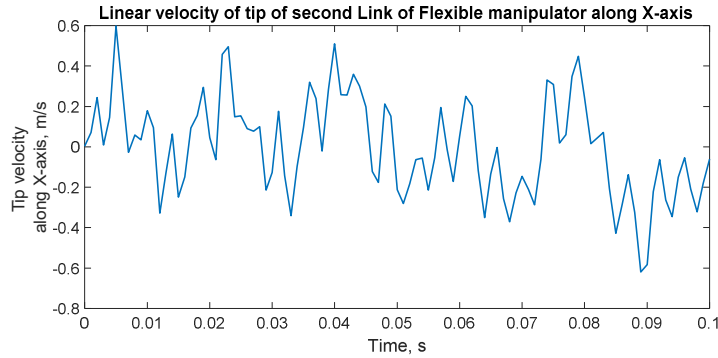**Linear velocity of tip of second Link of Flexible manipulator along Z-axis**
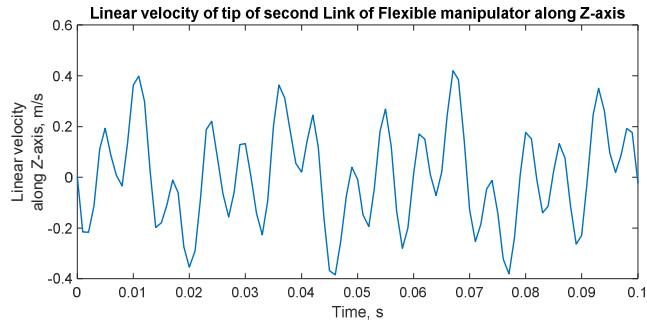
Fig. 9: Linear velocity of tip of second *flexible link* along Z-axis

Angular velocity of tip of second Link of Flexible manipulator about Y-axis
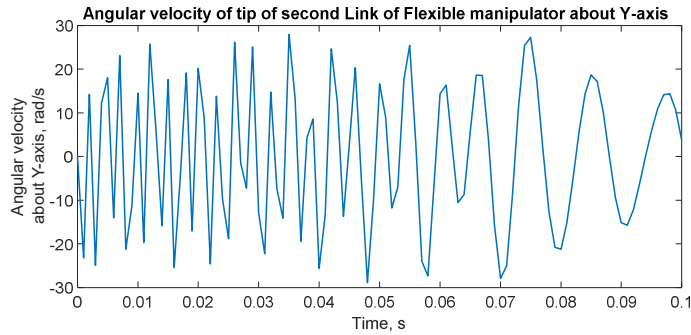
Fig. 10: Angular velocity of tip of second *flexible link* about Y-axis

Linear velocity of tip of second Link of Flexible manipulator along Y-axis

Fig. 11: Linear velocity of tip of second *flexible link* along Y-axis

Angular velocity of tip of second Link of Flexible manipulator about X-axis

Fig. 12: Angular velocity of tip of second *flexible link* about X-axis
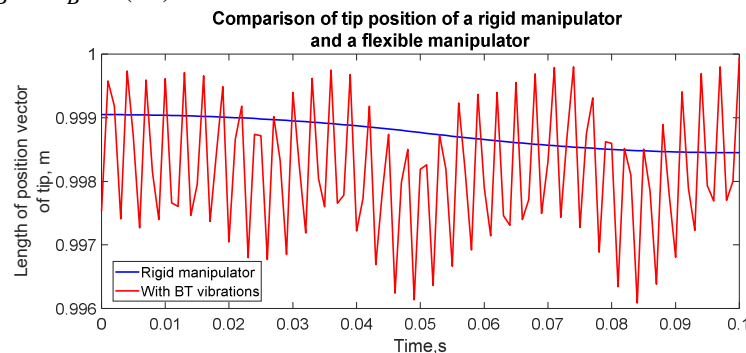
Fig. 13: Linear velocity of tip of second *flexible link* along X-axis

The undamped tip responses of second *flexible link* are shown in Fig. 8 to Fig. 13. From above graphs, it can be observed that the angular velocity about Z-axis (Fig. 8) is the maximum while the linear velocity about Y-axis (Fig. 11) is the maximum.

4.4 Effect of vibrations on positional accuracy

Now, the effect of vibration of *flexible links* on the positional accuracy of the end point of the second *link* (point B in Fig. 6) will be shown. The physical parameters provided in Table 2 are taken for the simulation. The length of the position vector of point B is given by 'OB'. It can be found out as follows:

$$OB = \sqrt{X_B^2 + Y_B^2 + Z_B^2} \quad (16)$$

X_B, Y_B and Z_B are the coordinates of point B (Fig. 6) w.r.t. ground frame XYZ (Fig. 1 and Fig. 2). These coordinates are calculated using equation (2). Fig. 14 shows the variation of length of position vector OB for a Two-Link Rigid manipulator and a Two-Link Flexible manipulator undergoing both bending and torsional vibrations. It is to be noted that the *rigid* manipulator operates in X-Y plane only. Hence, its Z-coordinate remains zero throughout. But for the *flexible* manipulator, due to presence of torsional vibrations, the *links* show some deflections in Y-Z plane also. Hence, the *flexible* manipulator undergoing both bending and torsional vibrations, no longer remains planar.


Fig. 14: Comparison of length of position vectors of the tip of second Link for a Two-Link Rigid and Flexible manipulators (The *flexible* manipulator undergoes coupled bending and torsional undamped vibrations; BT means Bending-Torsion).

In Figure 14 and Figure 15, BT stands for 'Bending-Torsion'. Figure 15 shows the three-dimensional plot of position of tip B (Fig. 6) of the *flexible* manipulator. When only bending vibrations are present, the *flexible* manipulator remains in X-Y plane, i.e., it can be said to be planar.
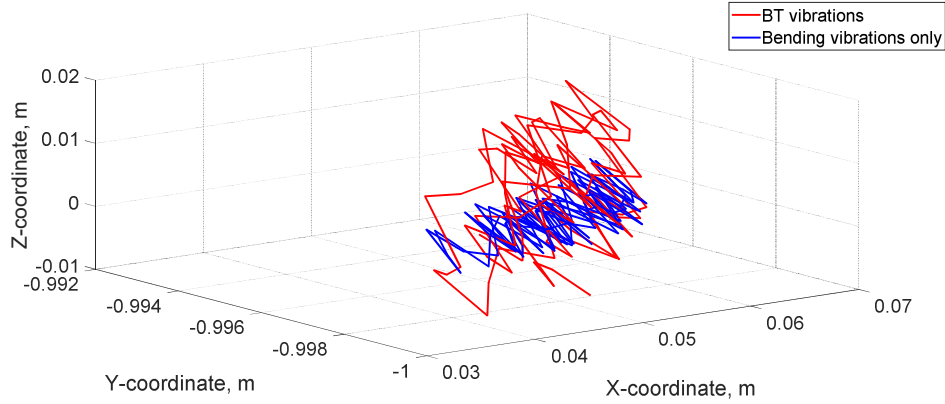
Fig.15: 3D-plot showing the position of tip of second Flexible Link for undamped vibrations.

In figure 15, the red coloured graph is for the *flexible* manipulator undergoing coupled bending-torsional (BT) vibrations while the blue coloured graph is for the *flexible* manipulator undergoing only bending vibrations. It is clear from the figure that presence of torsional vibrations severely deteriorates the positional accuracy of the tip B.

### 4.4.1 Frequency analysis of undamped vibrations of Flexible Links

Table 3 gives the natural frequencies of the Two-link Flexible manipulator for two finite elements (FEs) and ten finite elements (FEs).

Table 4: Natural frequencies of Flexible Manipulator

S. No.	Natural Frequency (using FEM)	
	2 FEs	*10 FEs*
1	1.6	2.05
2	2.1	2.07
3	5.7	6.99
4	7.1	7.00
5	27.5	19.9
6	35.3	20.5
7	56	39.6
8	71	42.6
9	1019	60.46
10	1497	67.3
11	1646.5	98.6
12	4229.4	112.9
13	-	132.07
14	-	153.79
15	-	175.52
16	-	184.78
17	-	245.2
18	-	248.3
19	-	302.87
20	-	336.13
21	-	391.53
22	-	425.97
23	-	449.47
24	-	462.91
25	-	508.78
26	-	587.4
27	-	592.88
28	-	651.24
29	-	705.69
30	-	779.52

Above frequencies were matched using FFT analyses. Fig. 16 to Fig. 18 show the FFT of the vibration of tip B of the *flexible* manipulator undergoing coupled bending-torsional vibrations.
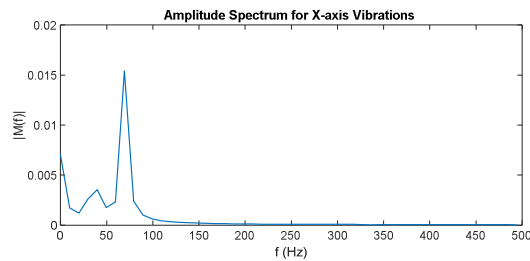
Fig. 16: FFT analysis of X-axis vibrations of tip B

From Fig. 16, it is found that the dominant frequencies are about: 40 Hz (near to 42.6 Hz in Table 4, column 3) and 70 Hz (near to 67.3 Hz in Table 4, column 3).
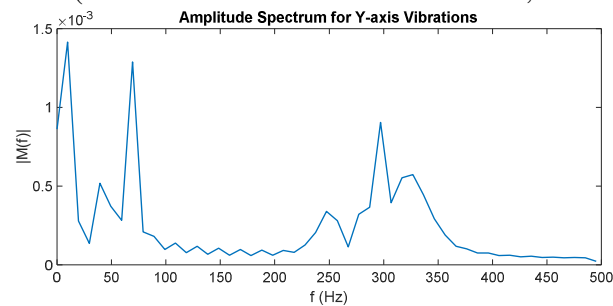
Fig. 17: FFT analysis of Y-axis vibrations of tip B

From Fig. 17, it is found that the dominant frequencies are about: 7 Hz (7 Hz in Table 4, column 3), 70 Hz (near to 67.3 Hz in Table 4, column 3) and 300 Hz (near to 302.87 Hz in Table 4, column 3). All these frequencies are present in Table 3. Besides that, other identifiable frequencies are about: 40 Hz (near to 39.6 Hz in Table 4, column 3) and 250 Hz (near to 248.3 Hz in Table 4, column 3). There are very small peaks between 100 Hz to 200 Hz. All these frequencies can be identified to be present in Table 3.
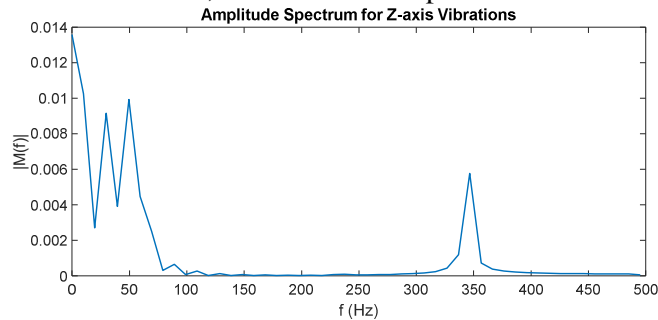
Fig. 18: FFT analysis of Z-axis vibrations of tip B

From Fig. 18, the dominant frequencies are about: 35 Hz (near to 39.6 Hz in column 3 and 35.3 Hz in column 2 in Table 4), 56 Hz (near to 56 Hz in column 2 and 60.46 Hz in column 3 in Table 4) and 350 Hz (near to 336.13 Hz in column 3, Table 4). The accuracy of FFT analysis depends upon the sampling frequency and sample size. For the present case, the sampling frequency is 1000 samples per second and sample size is 100.

5. VALIDATION OF MATHEMATICAL MODEL

The validation of mathematical model is done with the results of [24]. The physical parameters are given in Table 5.

444

Table 5: Physical parameters (as used by Chiaming et. al.) for validation

| Physical parameters	Values
Length of each *link*	$L_1 = L_2 = 1$ m
Mass of each *link*	$m_1 = m_2 = 5$ kg
Young's modulus	$E_1 = E_2 = 2 \times 10^{11}$ N/m^2
Second moment of area	$I_1 = I_2 = 5 \times 10^{-9}$ N/m^2
Initial conditions	$\theta_1 = 0^0$; $\theta_2 = 5^0$
Joint 1 torque	0 Nm
Joint 2 torque	Half sine wave of amplitude 2 Nm and duration 1 second.

The simulation results are shown in Fig. 19-21. To obtain these results, two finite elements are used during simulation, i.e., one finite element per *link*. The first two lowest frequencies of the *flexible* manipulator are found out to be: 2 Hz and 12 Hz.
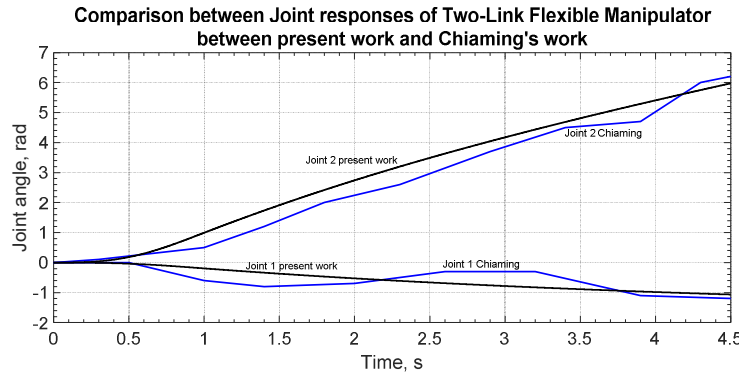

Fig. 19: Comparison of *joint* responses of Two-Link Flexible manipulator between present work and Chiaming's work

Figure 19 shows the *joint* responses of the *flexible* manipulator. These are compared with the results of Chiaming. It is found that the *joint* responses found in present work are close to the *joint* responses obtained by Chiaming.
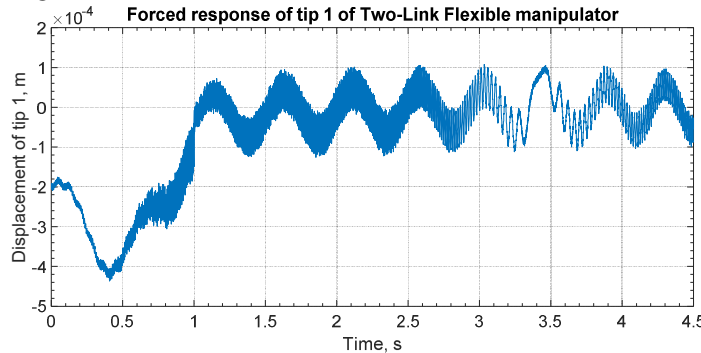
Fig. 20: Tip displacement of Link-1 of the Flexible manipulator
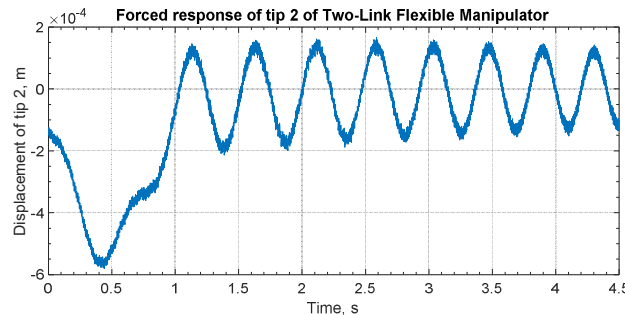
Fig. 21: Tip displacement of Link-2 of the Flexible manipulator

Figure 20 shows the tip displacement of Link-1 along global Y-axis and Fig. 21 shows the tip displacement of Link-2 along global Y-axis. It is found that the forced response (between 0 to 1 second) of the tips match well with the results of Chiaming but the transient responses do not match. In the present work, the transients exhibit the frequency of 2 Hz while in the work

of Chiaming, the transients exhibit the frequency of less than 2 Hz. It is notable that for the parameters of the *flexible* manipulator given in Table 5, the lowest natural frequency is found out to be 2 Hz which is same as being exhibited by the graphs in Figure 20 and Figure 21.

6. CONCLUSIONS

In this paper, Lagrangian-finite element method is used to obtain the dynamic model of a Two-Link Flexible manipulator. Two types of finite elements are considered for discretization of the *flexible links*. These are: 'space frame element' and 'plane frame element'. Coupling between *rigid* and *flexible* degrees of freedom is considered and its effect on simulation is shown. It is found that this coupling makes the system highly non-linear and the solutions to the equations of motion do not converge. In order to obtain results, the equations of motion are modified suitably and discussed within the paper. The effect of non-linearity due to the presence of centrifugal, Coriolis and gravity terms are also shown in the paper. The novelty of the paper lies in inclusion of torsional vibrations of the *links* along with the flexural vibrations. It is shown that due to the presence of torsional effect, the *flexible* manipulator no longer remains planar. The torsional vibrations severely deteriorate the positional accuracy of the manipulator.

REFERENCES

[1] Benosman and Vey, *Control of flexible manipulators: A survey*, Robotica, Vol 22, pp. 533-534, 2004.

[2] S. K. Dwivedy, Peter Eberhard, *Dynamic analysis of flexible manipulators, a review*, Mechanism and Machine Theory, pp. 749-777, 2006.

[3] Sunada and Dubowsky, *The application of finite elements methods to the dynamic analysis of flexible spatial and co-planar linkage systems*, Journal of Mechanical Design, Vol 103, pp. 643-651, 1981.

[4] Dado and Soni, *A generalized approach for forward and inverse dynamics of elastic manipulators*, IEEE, pp. 359-364, 1986.

[5] Nagnathan and Soni, *Non-linear flexibility studies for spatial manipulators*, IEEE, pp. 373-378, 1986.

[6] Usoro, Nadira, Mahil, *A Finite Element/ Lagrange approach to modelling lightweight flexible manipulators*, Journal of Dynamic Systems, Measurement and Control, Vol. 108, pp. 198-205, 1986.

[7] E. Bayo, *A finite-element approach to control the end-point motion of a single-link flexible robot*, Journal of Robotic Systems, Vol. 4, pp. 63-75, 1987.

[8] Simo and Vu-Quoc, *The role of nonlinear theories in transient dynamic analysis of flexible structures*, Journal of Sound and Vibration, Vol. 4, pp. 63-75, 1987.

[9] Tzou and Wan, *Distributed structural dynamics control of flexible manipulators-I, Structural dynamics and distributed viscoelastic actuator*, Computers & Structures, pp. 669-677, 1990.

[10] Chedmail, Aoustin and Chevallereau, *Modelling and control of flexible robots*, International Journal for Numerical Methods in Engineering, Vol. 32, pp. 1595-1619, 1991.

[11] Alberts, Xia, Chen, *Dynamic analysis to evaluate viscoelastic passive damping augmentation for the space shuttle remote manipulator system*, Journal of Dynamic Systems, Measurement and Control, Vol. 114, pp. 468-475, 1992.

[12] Gaultier and Cleghorn, *A spatially translating and rotating beam finite element for modelling flexible manipulators*, Mechanism and Machine Theory, Vol. 27, pp. 415-433, 1992.

[13] Hu and Ulsoy, *Dynamic modeling of constrained flexible robot arms for controller design*, Journal of Dynamic Systems, Meadurement and Control, Vol. 116, pp. 56-65, 1994.

[14] Stylianou and Tabarrok, *Finite element analysis of an axially moving beam, Part I: Time integration*, Journal of Sound and Vibration, Vol. 178, pp. 433-453, 1994.

446

[15] Stylianou and Tabarrok, *Finite element analysis of an axially moving beam, Part II: Stability analysis*, Journal of Sound and Vibration, Vol. 178, pp. 455-481, 1994.

[16] Theodore and Ghosal, *Robust control of multilink flexible manipulators*, Mechanism and Machine Theory, Vol. 38, pp. 367-377, 2003.

[17] R. Fotouhi, *Dynamic analysis of very flexible beams*, Journal of Sound and Vibration, Vol. 305, pp. 521-533, 2007.

[18] Meghdari and Ghassempouri, *Dynamics of Flexible Manipulators*, Journal of Engineering, Islamic Republic of Iran, Vol. 7, pp. 19-32, 1994.

[19] Theodore and Ghosal, *Comparison of the assumed modes method and finite element models for flexible multilink manipulators*, The International Journal of Robotics Research, Vol. 14, 1995.

[20] Chandrupatla and Belegundu, *Introduction to Finite Elements in Engineering*, New Delhi: PHI Learning Private Limited, Third Edition.

[21] Natraj Mishra, S.P. Singh, B.C. Nakra, *Dynamic Modelling of Two Link Flexible Manipulator using Lagrangian Assumed Modes Method*, Global Journal of Multidisciplinary Studies, Vol.-4, Issue-12, pp. 93-105, 2015.

[22] D. R. Bland, *The Theory of Linear Viscoelasticity*, London: Pergamon Press, 1960.

[23] S. Rao, *Mechanical Vibrations*, Pearson, Fourth Edition.

[24] Chiaming Yen, Glenn Y. Masada, Wei-Min Chan, *Dynamic Analysis of a Two-link Flexible Manipulator System using Extended Bond Graphs*, Journal of the Franklin Institute, Vol. 330, No. 6, pp. pp. 1113-1134, 1993.

[25] W. Chen, *Dynamic modeling of multi-link flexible robotic manipulators*, Computers & Structures, pp. 183-195, 2001.
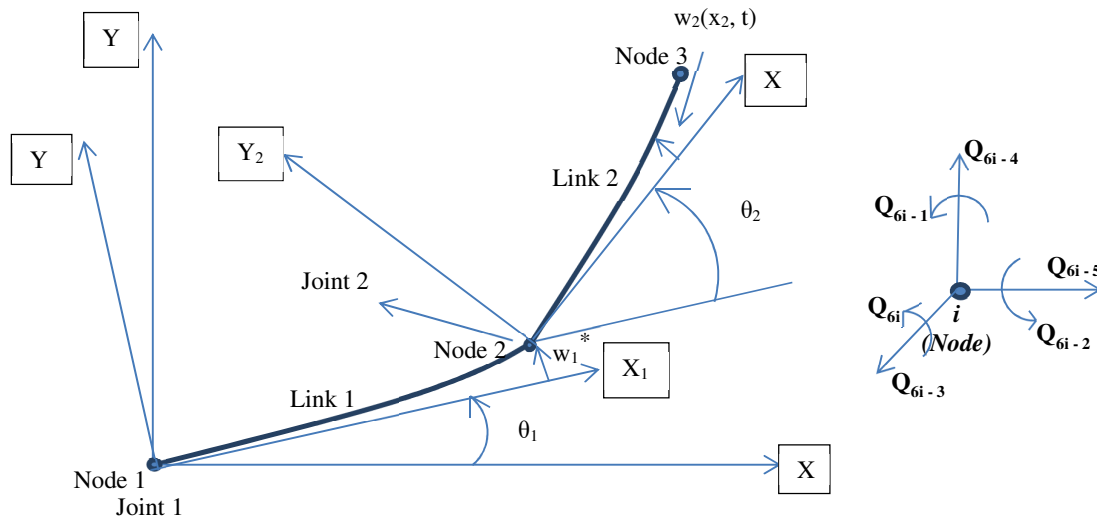
Fig. 2: Dynamics modelling of Two-Link Flexible manipulator using two Space-frame finite elements.

$$m_e' = \begin{bmatrix} m_{11e}' & m_{12e}' \\ m_{21e}' & m_{22e}' \end{bmatrix} \qquad (8e)$$

$$m_{11e}' = \begin{bmatrix} 2\mu_3 & 0 & 0 & 0 & 0 & 0 \\ 0 & 156\mu_1 & 0 & 0 & 0 & 22l_e\mu_1 \\ 0 & 0 & 156\mu_2 & 0 & 22l_e\mu_2 & 0 \\ 0 & 0 & 0 & 2\mu_4 & 0 & 0 \\ 0 & 0 & 22l_e\mu_2 & 0 & 4l_e^2\mu_2 & 0 \\ 0 & 22l_e\mu_1 & 0 & 0 & 0 & 4l_e^2\mu_1 \end{bmatrix};$$

$$m'_{12e} = \begin{bmatrix} \mu_3 & 0 & 0 & 0 & 0 & 0 \\ 0 & 54\mu_1 & 0 & 0 & 0 & -13l_e\mu_1 \\ 0 & 0 & 54\mu_2 & 0 & -13l_e\mu_2 & 0 \\ 0 & 0 & 0 & \mu_4 & 0 & 0 \\ 0 & 0 & 13l_e\mu_2 & 0 & -3l_e^2\mu_2 & 0 \\ 0 & 13l_e\mu_1 & 0 & 0 & 0 & -3l_e^2\mu_1 \end{bmatrix}$$

$$m'_{21e} = \begin{bmatrix} \mu_3 & 0 & 0 & 0 & 0 & 0 \\ 0 & 54\mu_1 & 0 & 0 & 0 & 13l_e\mu_1 \\ 0 & 0 & 54\mu_2 & 0 & 13l_e\mu_2 & 0 \\ 0 & 0 & 0 & \mu_4 & 0 & 0 \\ 0 & 0 & -13l_e\mu_2 & 0 & -3l_e^2\mu_2 & 0 \\ 0 & -13l_e\mu_1 & 0 & 0 & 0 & -3l_e^2\mu_1 \end{bmatrix}$$

$$m'_{22e} = \begin{bmatrix} 2\mu_3 & 0 & 0 & 0 & 0 & 0 \\ 0 & 156\mu_1 & 0 & 0 & 0 & -22l_e\mu_1 \\ 0 & 0 & 156\mu_2 & 0 & -22l_e\mu_2 & 0 \\ 0 & 0 & 0 & 2\mu_4 & 0 & 0 \\ 0 & 0 & -22l_e\mu_2 & 0 & 4l_e^2\mu_2 & 0 \\ 0 & -22l_e\mu_1 & 0 & 0 & 0 & 4l_e^2\mu_1 \end{bmatrix}$$

In above matrices, $\mu_1 = \mu_2 = \frac{\rho A_e l_e}{420}; \mu_3 = \frac{\rho A_e l_e}{6}; \mu_4 = \frac{J_m}{6}$ (8f)

where, ρ = mass density of the element, and J_m = mass moment of inertia of the element.

$$f' = \begin{bmatrix} 0 & \frac{p_z l_e}{2} & \frac{p_y l_e}{2} & 0 & \frac{-p_z l_e^2}{12} & \frac{p_y l_e^2}{12} & 0 & \frac{p_z l_e}{2} & \frac{p_y l_e}{2} & 0 & \frac{p_z l_e^2}{12} & \frac{-p_y l_e^2}{12} \end{bmatrix}^T \quad (8g)$$

where, p_y and p_z are the distributed loads on the element along y- and z-directions respectively.

$$For\ Link-1, f' = \begin{bmatrix} 0 & \frac{p_z l_e}{2} & \frac{p_y l_e}{2} & 0 & \frac{-p_z l_e^2}{12} & \frac{p_y l_e^2}{12} & 0 & \frac{p_z l_e}{2} & \frac{p_y l_e}{2} & 0+T_{w1} & \frac{p_z l_e^2}{12}+GC_1 & \frac{-p_y l_e^2}{12}-\tau_1 \end{bmatrix}^T \quad (15c)$$

$$For\ Link-2, f' = \begin{bmatrix} 0 & \frac{p_z l_e}{2} & \frac{p_y l_e}{2} & 0 & \frac{-p_z l_e^2}{12} & \frac{p_y l_e^2}{12} & 0 & \frac{p_z l_e}{2} & \frac{p_y l_e}{2} & 0 & \frac{p_z l_e^2}{12}+GC_2 & \frac{-p_y l_e^2}{12}-\tau_1-\tau_2 \end{bmatrix}^T \quad (15d)$$
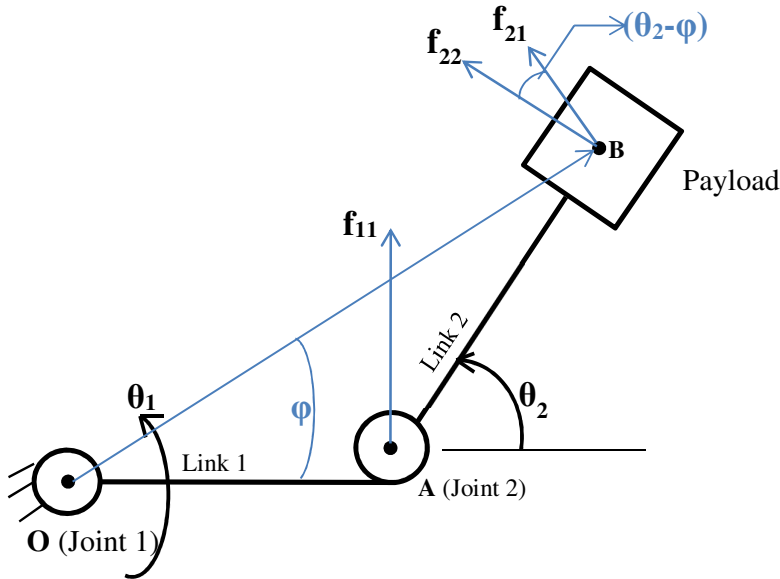

Fig. 6: Calculation of excitation forces at the ends of *links*

ANALIZA DINAMICĂ A MANIPULATORULUI FLEXIBIL CU DOUĂ LEGĂTURI FOLOSIND FEM ÎN CURS DE ÎNDOIRE-TORSIUNE VIBRAȚII

Rezumat: În această lucrare, un manipulator flexibil cu două legături este analizat folosind o abordare cu elemente finite ale cărei legături sunt în curs de îndoire combinată și vibrații de torsiune. Modelul matematic al manipulatorului flexibil se obține folosind dinamica lagrangian. Link-urile sunt modelate ca grinzi Euler-Bernoulli și discretizate folosind "spațiu-cadru" și "plan-cadru" elemente. Lucrarea prezentă tratează diverse efecte neliniare ar fi, cuplarea între grade rigide și flexibile de libertate, efecte centrifuge și Coriolis și prezența gravitației. Modelul matematic este validat folosind rezultatele disponibile în literatura de specialitate. Noutatea prezentei lucrări constă în includerea efectelor torsionale și evidențiind astfel efectele acestora asupra preciziei poziționale a manipulatorului flexibil.

Natraj MISHRA, Assistant Professor, School of Engineering, UPES Dehradun, India, Email: natrajmishra@gmail.com

S.P. SINGH, Professor, Department of Mechanical Engineering, IIT Delhi, India, Email: spsingh100@gmail.com